Research Article

Angga Kengkongan Ary, Yuwana Sanjaya, Aditya Rio Prabowo*, Fitrian Imaduddin, Nur Azmah Binti Nordin, Iwan Istanto, and Joung Hyung Cho

Numerical estimation of the torsional stiffness characteristics on urban Shell Eco-Marathon (SEM) vehicle design

https://doi.org/10.1515/cls-2021-0016
Received Dec 06, 2020; accepted Mar 12, 2021

Abstract: Shell Eco-Marathon (SEM) is an international competition among university students that involves designing, building, and driving energy-efficient cars. The car frame is the most crucial aspect influencing the strength of the car. This research aims to obtain maximum torsional strength with variations in the material and thickness of the frame. Calculation and testing are done using the simulation method to obtain a strong car frame. This simulation method is calculated by a series of finite element analyses. Then, data from the simulation method are obtained in the form of deformation and safety factors. By comparing the moment received with its deformation, torsional stiffness is then obtained. Furthermore, the torsional stiffness is divided by the weight to produce a value ratio. It is known that the factor which has the most significant influence on the difference in torsional stiffness of each variation is the shear modulus of the material used. In contrast, the weight of the chassis is influenced by the density of the material and the thickness of the chassis. Additionally, the safety factor of each variation is strongly influenced by the strength of the chassis structure itself. The results of this study will demonstrate the car frame design with the best performance.

Keywords: torsional stiffness, Shell Eco-Marathon, frame ladder, weight, finite element analysis

1 Introduction

The main things that must be considered when designing a vehicle are safety, driving comfort, and traction power when it is driven, with the efficient use of as little fuel as possible as an appropriate model for city traffic [1]. One explanation for why vehicles produce toxic exhaust emissions is the incomplete combustion process [2]. The use of refrigerants influences and increases global warming, meaning that people are increasingly encouraged to look for alternative refrigeration systems that are more environmentally friendly, safe, and can be used continuously in the future [3]. Shell Eco-Marathon (SEM) is a unique global program where university students design, build, and drive highly energy-efficient cars. Students around the world collaborate to find innovative solutions to improve energy efficiency, aligning with Shell's goals and commitment to developing a cleaner energy solution together [4]. SEM vehicles must be lightweight and able to hold the load given, both when driving on a straight track and when turning [5]. As shown in Figure 1, SEM vehicles are run to the time of competition to produce minimum fuel consumption, which is indicated by kilometers per liter. The most important factors are weight, aerodynamic drag, wheel and bearing friction, and, last but not least, power efficiency [6].

Figure 1: Urban Shell-Eco Marathon vehicle design

***Corresponding Author: Aditya Rio Prabowo:** Department of Mechanical Engineering, Universitas Sebelas Maret, Surakarta 57126, Indonesia; Email: aditya@ft.uns.ac.id
Angga Kengkongan Ary, Yuwana Sanjaya, Fitrian Imaduddin: Department of Mechanical Engineering, Universitas Sebelas Maret, Surakarta 57126, Indonesia
Nur Azmah Binti Nordin: Malaysia-Japan International Institute of Technology – University Teknologi Malaysia, Kuala Lumpur 54100, Malaysia
Iwan Istanto: Agency for the Assessment and Application of Technology, Jakarta 10340, Indonesia
Joung Hyung Cho: Department of Industrial Design, Pukyong National University, Busan 48513, South Korea

The frame is the most crucial part of the vehicle because it must be strong enough to hold other components of the car, such as the engine, fuel tank, braking system, steering system, and suspension system [7]. The frame must also be able to protect the driver from accidents in the event of car crashes or overturns [8], in which the frame has high strength and stiffness, with low weight and cost. Conversely, a weak frame will make the vehicle sensitive and difficult to drive [9]. Calculations and testing to determine the strength and stiffness of the SEM vehicle are not simple because the shape of the frame itself is different from the general frame [10]. Testing the strength and stiffness of the frame will provide information about torsional stiffness in the form of the relationship between the forms of the frame, the given load, and the deformation of the SEM vehicle frame. After obtaining this information, students can develop a frame with good strength and stiffness. High torsional stiffness is crucial for a frame because it will affect the overall vehicle performance [11]. One effect of good torsional stiffness on the frame is in the vehicle's ability to get maximum grip when turning at high speed, which is influenced by the balanced lateral force distribution to the four wheels [12]. A frame with excellent torsional stiffness will also make other vehicle components such as suspension systems and steering systems work optimally since the deformation of the twisting load can be ignored, thus resulting in a good suspension system and steering system, unaffected by the deformation of the frame [13].

Given the facts above, it is vital to assess the torsional stiffness of the vehicle design, including the recently developed urban Shell-Eco Marathon vehicle. Considering that the torsional stiffness calculation is yet to be conducted to the subject, this study addresses the numerical calculation of the torsional stiffness of the vehicle design under various component modifications. The results, in the form of the deformation and stiffness-to-weight ratio, are summarized, while the design with the best torsional stiffness characteristic is expected to be concluded in later discussion.

2 Benchmarking study

This study uses static analysis of urban Shell Eco-Marathon (SEM) concept vehicles as a benchmark, which provides data from Autodesk Inventor simulations and manual calculations [14]. The design uses Aluminum 6061 hollows with a total dimension of 2060 × 600 mm. It consists of 7 support bars (25 × 25 mm) and two main bars (40 × 40 mm). There are three weights (driver's leg, driver's body, and engine) that are applied to the chassis in each part of the supporting rod. The estimated driver's foot has a load of 98.1 N and is supported by one supporting rod, whereas the driver's body, with a load of 294.3 N, is supported by two support bars. The machine has a load of 196.2 N, which is also supported by two support rods. Figure 2 shows the geometry of the vehicle chassis and load distribution. The ratios of manual calculations, Autodesk Inventor simulations, and ANSYS simulation are shown in Tables 1 to 3. It can be concluded that ANSYS provided good results. Similarity with analytical calculation was found in the lowest ratio of 44.50% in terms of displacement. However, besides this value, the other results are satisfactory, with the highest error being less than 11%.

The second benchmark method used is to vary the mesh size from 5 to 60 mm within the interval of 5 (see Table 4). The mesh size variation is applied within the driver's feet frame area. The driver's feet area is chosen because comparison between manual calculation and simulation has the most significant ratio compared to other parts of the frame. The parameters affected by differences in mesh

Table 1: Error comparison of the analytical calculations, rapid estimation (Autodesk Inventor) and ANSYS: machine components

Parameters	Analytical calculation	Rapid estimation	ANSYS	E_1 (%)	E_2 (%)
1st Principle Max. Stress (MPa)	8.48	7.80	6.975	17.75	10.58
Displacement (mm)	0.15	0.08	0.075	50	6.25
Safety Factor (-)	-	15	15	-	0.00

where E_1 is the error between analytical calculation and ANSYS, while E_2 is the error between rapid estimation and ANSYS.

Table 2: Error comparison of the analytical calculations, rapid estimation (Autodesk Inventor) and ANSYS: body part of the driver

Parameters	Analytical calculation	Rapid estimation	ANSYS	E_1 (%)	E_2 (%)
1st Principle Max. Stress (MPa)	12.7	11.71	8.866	30.19	24.29
Displacement (mm)	0.22	0.12	0.098	55.45	18.33
Safety Factor (-)	-	15	15	-	0.00

Table 3: Error comparison of the analytical calculations, rapid estimation (Autodesk Inventor) and ANSYS: part of driver leg

Parameters	Analytical calculation	Rapid estimation	ANSYS	E_1 (%)	E_2 (%)
1st Principle Max. Stress (MPa)	4.25	3.90	3.489	17.90	10.54
Displacement (mm)	0.07	0.04	0.038	45.71	5.00
Safety Factor (-)	-	15	15	-	0.00

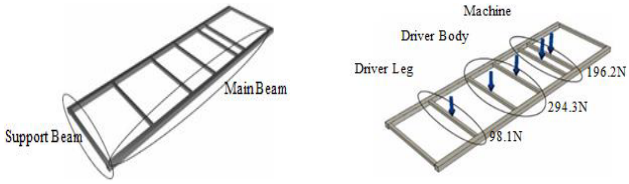

Figure 2: Shell Eco-Marathon (SEM) chassis and load distribution

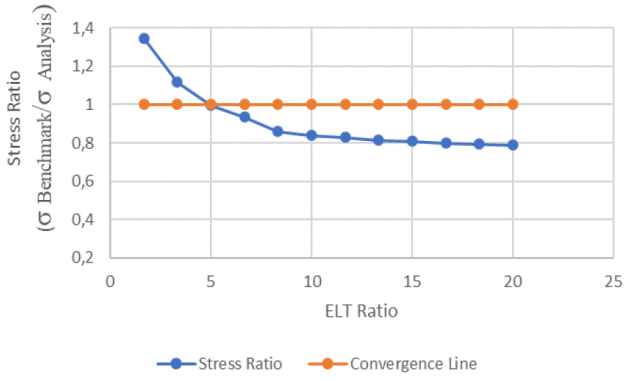

Figure 3: Mesh convergence study: observation to the stress behavior

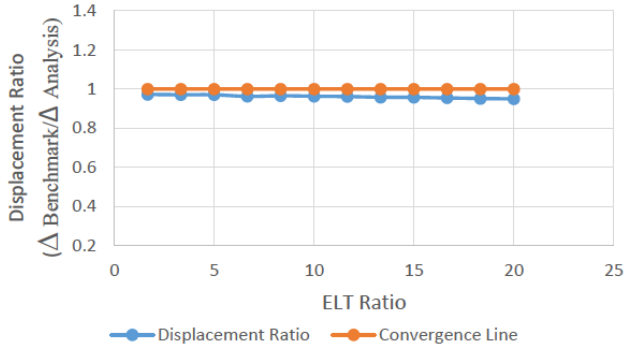

Figure 4: Mesh convergence study: observation to the displacement behavior

are nodes, elements, maximum stress results, and displacement. The mesh convergence study (Figures 3 and 4) with stress ratio is obtained by plotting the stress ratio with the element length to thickness (ELT) ratio; meanwhile, the mesh convergence study with displacement ratio was obtained by plotting the displacement ratio with the ELT ratio.

Table 4: Benchmark result of static analysis determined by the mesh variations

Mesh size (mm)	Maximum stress (MPa)	Displacement (mm)
5	5.2642	0.0389
10	4.3645	0.0389
15	3.8966	0.0388
20	3.6563	0.0385
25	3.3601	0.0386
30	3.2791	0.0385
35	3.2393	0.0385
40	3.1808	0.0383
45	3.1616	0.0383
50	3.1235	0.0382
55	3.1042	0.0381
60	3.0844	0.0380

3 Research methodology

3.1 Geometrical design

The primary purpose of the frame design is to ensure that all loads will be distributed through the meeting point of each part of the frame so that no force causes the frame to bend or be suppressed by bending loads [15]. To get a good frame design, it takes a balanced combination of strength and mass. This study discusses the comparative analysis between torsional stiffness to the mass of several skeletal variations. The frame of the SEM urban vehicle was arranged with a rectangular hollow profile with dimensions of 1×2 (inches), with the design shown in Figure 5 and the variations in Figure 6.

The frames had identical shapes, but had differences in the thickness and the type of material used. There were three sizes of frame thickness, which were 1.4, 0.9, and 0.4 mm. While the types of material used in the SEM vehicle frame were Aluminum 5052, Aluminum 6061, and Aluminum 7075, this research was then carried out with the steps shown in Figure 7.

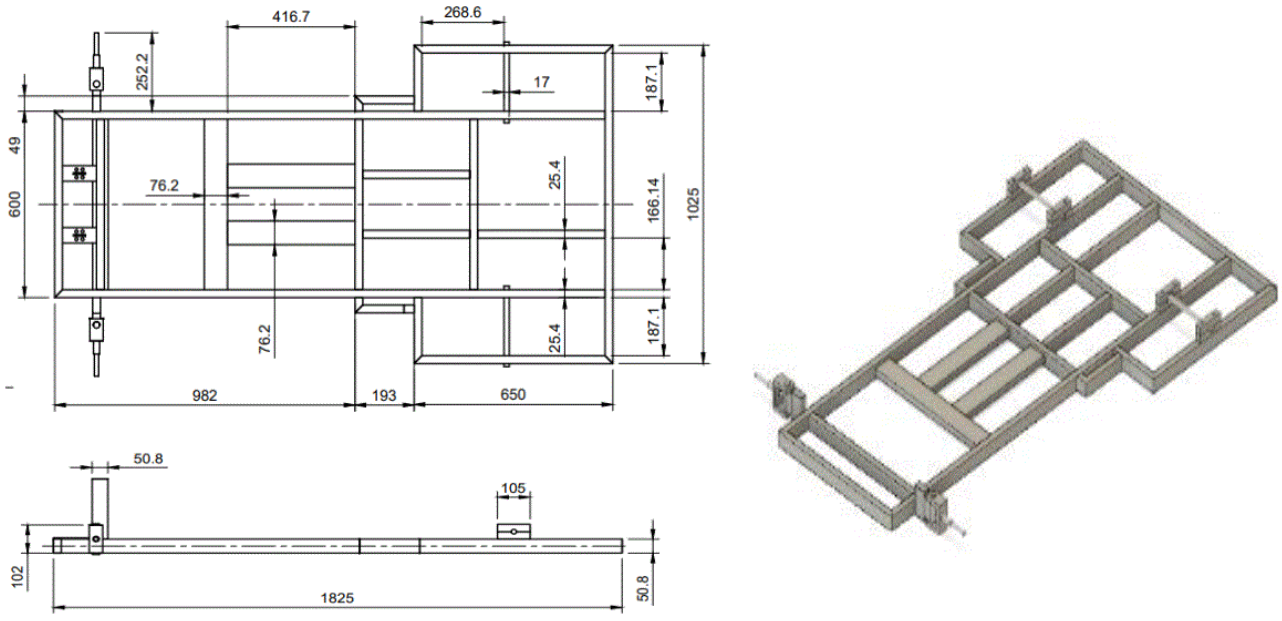

Figure 5: Design of SEM urban vehicle frames

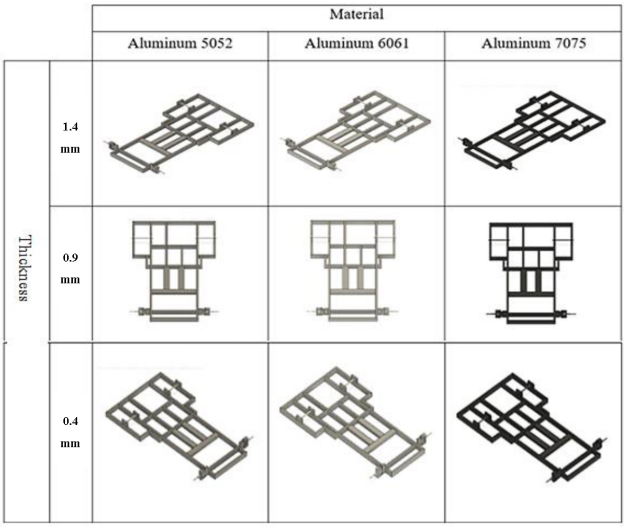

Figure 6: Variations in frame design for SEM urban vehicles

3.2 Applied material

The materials used for the SEM vehicle ladder frame in this study were Aluminum 5052, Aluminum 6061, and Aluminum 7075. These three materials have different properties, as shown in Tables 5 to 7.

3.3 Meshing configuration

All frame variations were simulated using the same meshing parameters, namely standard mechanical ten nodes

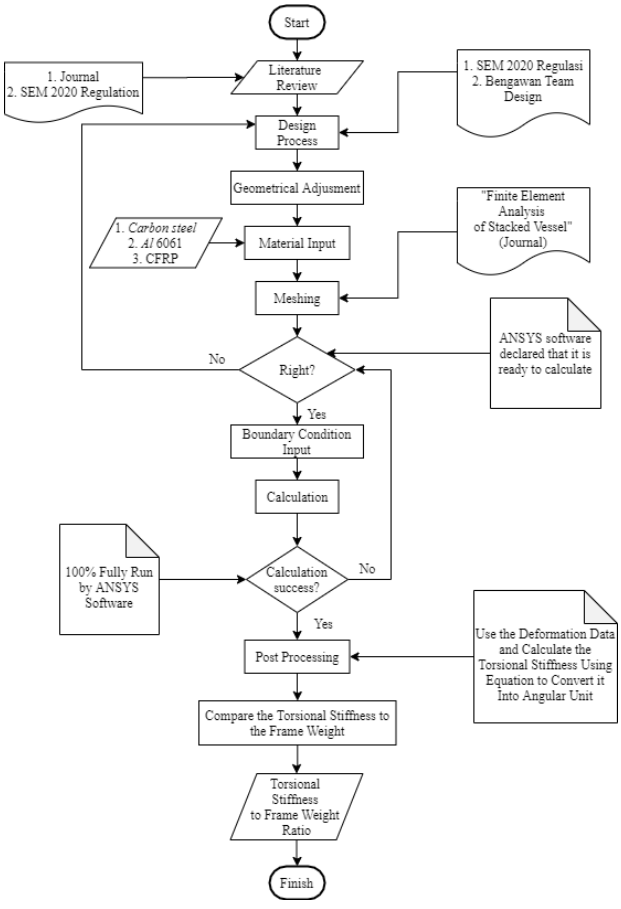

Figure 7: Research flow diagram

Table 5: Properties of the material Aluminum 5052

Parameter	Value
Shear Modulus	25924.2 MPa
Young's Modulus	70.3 GPa
Poisson's Ratio	0.35588
Density	2.68 g/cm^3
Yield Strength	193 MPa
Tensile Strength	228 MPa

Table 6: Properties of the material Aluminum 6061

Parameter	Value
Shear Modulus	25864 MPa
Young's Modulus	68.9 GPa
Poisson's Ratio	0.33197
Density	2.7 g/cm^3
Yield Strength	275 MPa
Tensile Strength	310 MPa

Table 7: Properties of the material Aluminum 7075

Parameter	Value
Shear Modulus	26900 MPa
Young's Modulus	71.7 GPa
Poisson's Ratio	0.33271
Density	2.81 g/cm^3
Yield Strength	145 MPa
Tensile Strength	276 MPa

tetrahedral shape with a transition ratio of 0.272, a maximum layer of 5, and a growth rate of 1.2. Other settings for meshing were set to default because different meshing densities are needed for each frame based on the shape, structure, and frame material itself [8]. The ten-node tetrahedral mesh form was chosen since it has an excellent ability to inform the shape of the curve despite the fewer nodes. Furthermore, its accuracy remains high with simpler, lighter, and faster calculations. Convergence is guaranteed only if there exists a static equilibrium path that connects the states of the solid at the start and end of a time increment [16]. The mesh size is designed based on the conclusions of the convergence study which the model has 282639 nodes and 137560 elements. In Figure 8, the result of the meshing carried out on the SEM urban vehicle frame design is shown.

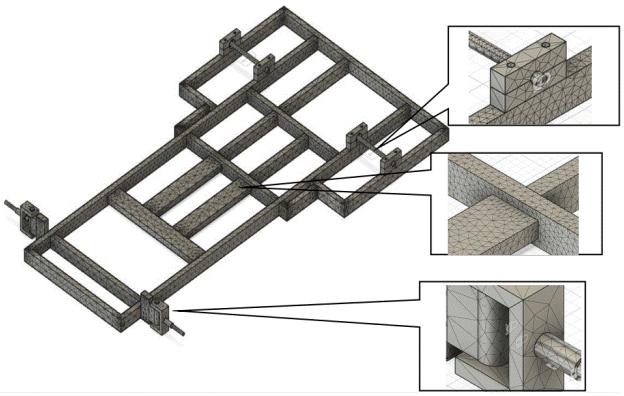

Figure 8: Meshing on the SEM urban vehicle frame design

3.4 Boundary condition

The boundary condition of this analysis was making the rear frame fixed so that the rear frame did not move. Consequently, the front frame was given a load in the opposite direction to form a twisting load [17]. The boundary conditions that were applied were based on the actual conditions of the vehicle, which can cause maximum torsional loads, namely when the vehicle maneuvers on a bend and when the car crosses uneven roads [17]. The force applied was 450 N on each side, assuming a vehicle weight of 180 kg distributed evenly on all four wheels and fixed support on the rear legs of the frame acting as the center of twisting.

The boundary conditions of simulation imposed twisting loads to the frame, where the loads were created by applying two forces, specifically to the front legs in the opposite direction, and to the rear legs being fixed. All frame variations had the same leg positions, both on the front and the rear end, and also had the same points of weight application. In this study, fixed support, also commonly known as structural constraint, was placed on the rear wheels, as shown in Figure 9.

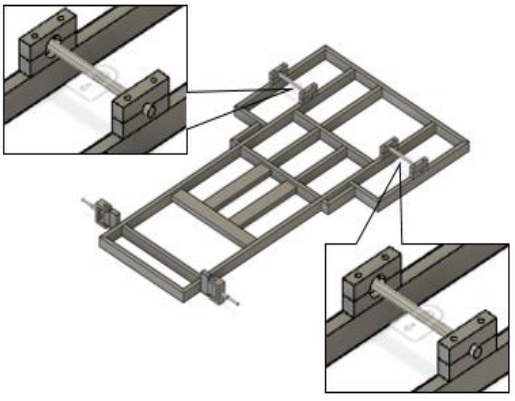

Figure 9: Structural constraints in the design of SEM urban vehicles

3.5 Fundamental equation

This research used a simulation of the frame design through the finite element method to produce data on the frame torsional stiffness. Torsional stiffness can also be calculated by applying the concept of physics, namely by placing a load on the front wheels and setting the rear wheel as fixed so that it does not move, causing the twisting load as desired. After that, changes to the structure in the form of the deformation of size and angle can be measured. Research from related journals used the following equations, *i.e.*, Eq. (1) to Eq. (5), to prove the results of the simulation analysis, which were then simulated again to be used as a reference.

$$T = m \times g \times L = (F_1 + F_2)\, w \tag{1}$$

$$\theta = \tan^{-1} \frac{a - b}{L} \tag{2}$$

$$K = \frac{T}{\theta} \tag{3}$$

$$K = \frac{G \times K_T}{L}, \tag{4}$$

$$K_T = a^4 \left[0,978 \left(\frac{T}{a} \right) - 2,309 \left(\frac{T}{a} \right)^2 + 1,826 \left(\frac{T}{a} \right)^3 \right]$$

$$\text{Torsional stiffness to weight ratio} = \frac{K}{m} \tag{5}$$

where:
T – Total torsion (Nm)
m – Mass (kg)
g – Gravity ($\text{m}\cdot\text{s}^{-2}$)
L – Length (m)
F_1 – Force 1 (N)
F_2 – Force 2 (N)
W – Distance from force to the center of the frame (m)
θ – Twist angle (deg)
A – Deformation on a side (m)
B – Deformation on b side (m)
K – Torsional Stiffness (Nm/deg)
G – Shear Modulus (MPa)
a – Maximum deformation (m).

4 Design analysis and scenario

The deformation results of the simulation occur in the parts where the legs are placed on the frame. Deformation in this section is seen by referring to the deformation color legend. These results are then calculated using the equation of torsional angle of the frame in angular units (degrees). The total torque equation is used to calculate the torque acting on the analyzed frame. Torsional stiffness obtained by comparing the moment received by the frame with its deformation Eq. (3). The last step is to compare the torsional stiffness obtained with the weight of the frame to get the value comparison between the two variables using Eq. (5). This ratio between torsional stiffness and the weight of the frame will be the reference value in this study in developing the frame.

4.1 Reference criteria for torsional stiffness of the SEM urban vehicle

Gawande [18] conducted a study to optimize torsional stiffness in a commercial heavy vehicle chassis using the finite element method. The chassis type is a ladder frame with a chassis thickness of 8 mm and a BSK46 material (G = 128.7 GPa), with a torsional stiffness of 282.93 MNm/rad. Kurisetty [19] calculated the torsional stiffness of the same type of chassis but with a different thickness of 6 mm with A36 steel material (G = 76.91 GPa), which results in a torsional stiffness value of 541 Nm/deg. Khoiron [20] also researched the same topic based on a similar chassis type with a 2 mm-thick profile and Al ENAW-6082T6 for the material (G = 27.3 GPa), which produced a torsional stiffness of 23.72 kNm/deg. He also researched a chassis with a thickness of 14 mm with carbon fiber material (G = 53 GPa), which produces a torsional stiffness of 50.88 kNm/deg. By analyzing the data from these references, the value of torsional stiffness for a good SEM urban vehicle can be determined. Therefore, with the trends obtained from the graph that can be seen in Figures 10 and 11, the value of torsional stiffness for SEM urban vehicles can be calculated based on the influence of thickness and shear modulus, which is 3.88 and 4.85 kNm/deg, respectively.

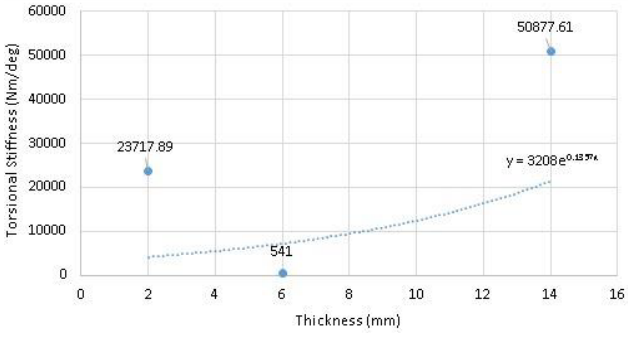

Figure 10: Effect of chassis thickness on torsional stiffness

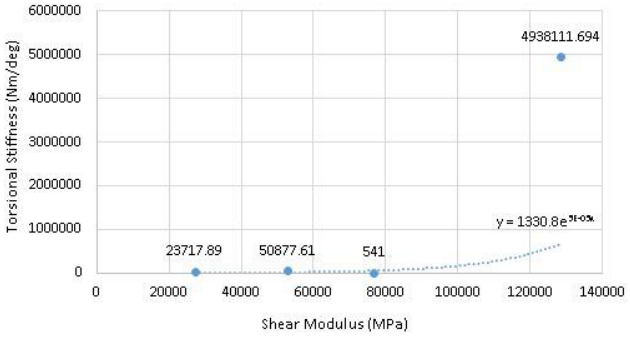

Figure 11: Effect of shear modulus on torsional stiffness

4.2 Designed analysis

A ladder frame chassis is a type of designed chassis. The basic principle of chassis design is to have high torsional stiffness with a light weight to get excellent handling performance on the car as well as low fuel consumption. Torsional stiffness is the ability of the chassis to withstand twisting loads in the form of the torque needed to twist the chassis 1 degree. When turning, if the torsional stiffness is too small, the chassis will fail. If it is too large, it will be difficult to turn and tend to under-steer. The results of the torsional ladder frame stiffness are different from other types of chassis because of the difference in construction structure. Ladder frames were chosen because they are lightweight, inexpensive, require simple tools in manufacturing, and can be easily repaired in cases of chassis damage [21]. Torsional stiffness is strongly influenced by the shape of the chassis structure, material, and the method of connecting the chassis [22]. In this study, the three variations of the frame have different materials, namely Aluminum series 5, series 6, and series 7, with the same connection method, specifically tungsten inert gas (TIG) welding. Therefore, this research focuses on comparing each chassis variation with a variety of material types and profile thicknesses of the chassis.

The purpose of this chassis design is to obtain a chassis with a torsional stiffness to weight ratio value that is higher than the available variations. An analysis of deformation and safety factors is carried out for each chassis variation with changes in the type of material and thickness of the chassis to achieve those objectives [22]. A deformed chassis will be vulnerable to fatigue failure because the twisting load will be experienced continuously by the frame while driving on the track. Suspension settings can be done to reduce the twisting load applied to the chassis. If the chassis can handle twisting loads properly, other loads such as bending will not be a problem [15]. The design process begins with an analysis of the Shell Eco-Marathon 2019 Official Rules [22]. The second step is determining the required performance criteria, such as torsional stiffness and minimum safety factor. Then, we determine the position of the engine, differential, legs, pedals, and other aspects. After obtaining the required data, we proceed with sketching and three-dimensional modelling. After designing the chassis under the targets and regulations, the frame is made.

The first to third variations of the chassis use Al 5052 material type with a thickness of 0.4, 0.9, and 1.4 mm. The fourth, fifth, and sixth variations use the Al 6061 material with a thickness of 0.4, 0.9, and 1.4 mm, respectively. Then, the seventh, eighth, and ninth variations use the 7075 type of material with a thickness of 0.4, 0.9, and 1.4 mm. By varying the thickness of the chassis on the same type of material, we found differences in chassis weight of about 2 kg. In comparison, the application of variations in the type of material at the same chassis thickness obtained a difference in chassis weight that is not significantly less than 1 kg (see Table 8).

Table 8: List of the chassis weight

Variation	Weight (kg)
1 (Al5 0.4)	5.110
2 (Al5 0.9)	7.434
3 (Al5 1.4)	9.638
4 (Al6 0.4)	5.148
5 (Al6 0.9)	7.489
6 (Al6 1.4)	9.710
7 (Al7 0.4)	5.358
8 (Al7 0.9)	7.794
9 (Al7 1.4)	10.110

5 Results and discussion

5.1 Structural deformation

The purpose of this simulation of torsional loading is to determine the chassis strength when subjected to torsional loads. The simulation results are the deformation and safety factor, where the deformation results, which are further analyzed, are the deformation on the front of the chassis being tested. Looking at the color of the first variation chassis and matching them with the legend (Figure 12), the maximum deformation is 3.005 mm, while the minimum deformation is 1.142 mm. The minimum safety factor on this chassis vari-

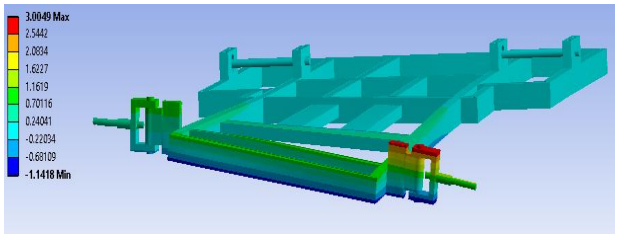

(a)

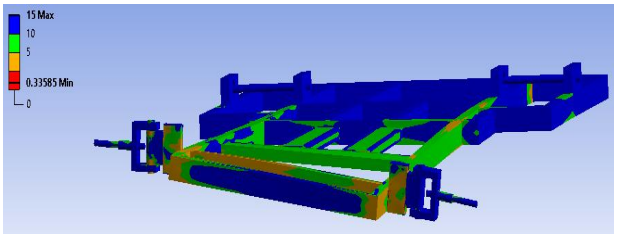

(b)

Figure 12: Deformation (a) and safety factor (b) of the first variation chassis simulation

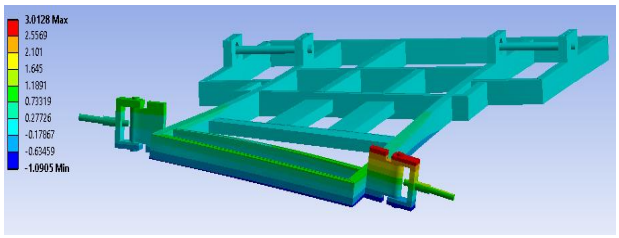

(a)

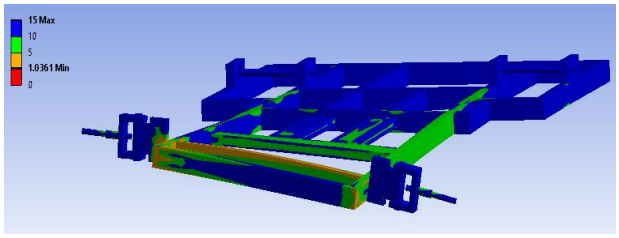

(b)

Figure 14: Deformation (a) and safety factor (b) of the third variation chassis simulation

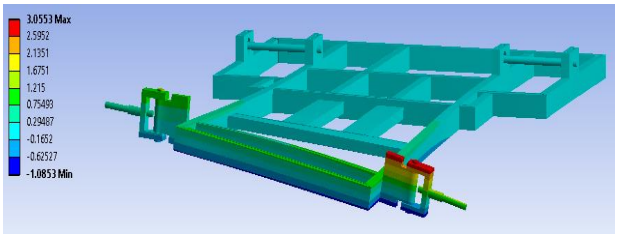

(a)

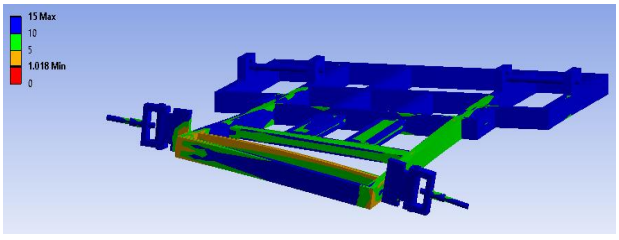

(b)

Figure 13: Deformation (a) and safety factor (b) of the second variation chassis simulation

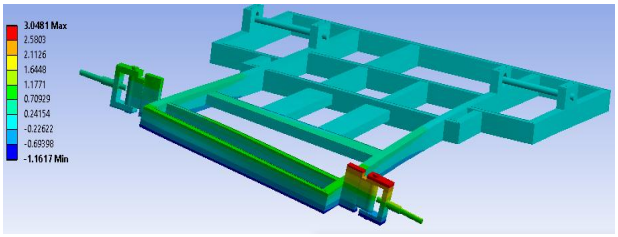

(a)

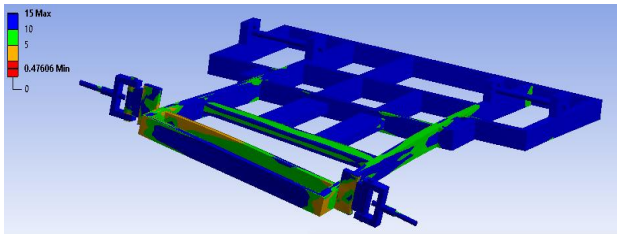

(b)

Figure 15: Deformation (a) and safety factor (b) of the fourth variation of chassis simulation

ation is 0.336, which is not strong enough, since it is below 1 [17].

As seen in Figure 13, the second variation of the chassis has a maximum deformation of 3.055 mm, while the minimum deformation is 1.085 mm. The minimum safety factor of this variation is 1.018, which is quite strong, since the deformation is still above the yield strength value.

In the third chassis variation (Figure 14), the maximum deformation is 3.013 mm, while the minimum deformation is 1.091 mm. The minimum safety factor of the chassis in this variation is 1.036, indicating that this chassis is also quite strong, given the deformation that is slightly above the yield strength.

In the fourth variation of the chassis, there is a maximum and minimum deformation of 3.048 and 1.162 mm, respectively (Figure 15). The minimum safety factor obtained is 0.476, which indicates this chassis is not strong enough, since the safety factor value is below 1.

In the fifth chassis variation (Figure 16), a maximum deformation of 3.104 mm and a minimum deformation of

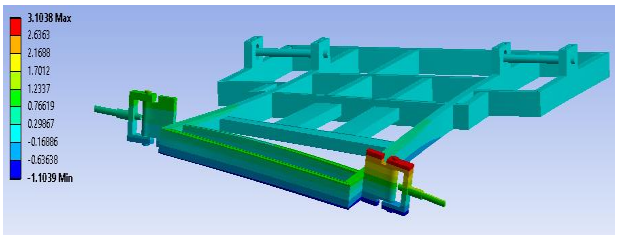

(a)

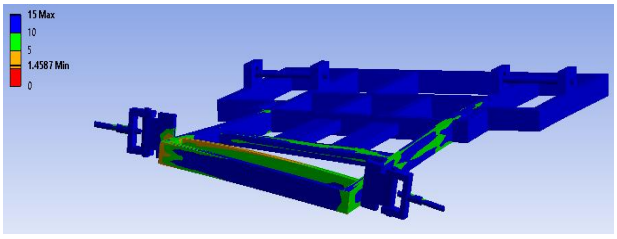

(b)

Figure 16: Deformation (a) and safety factor (b) factor of the fifth variation of chassis simulation

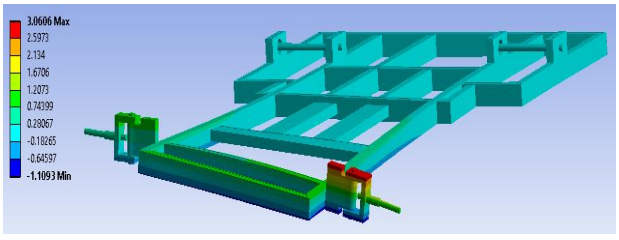

(a)

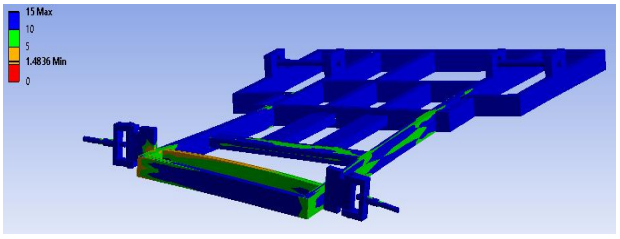

(b)

Figure 17: Deformation (a) and safety factor (b) of the sixth variation of chassis simulation

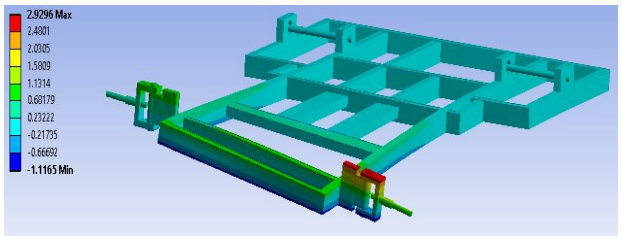

(a)

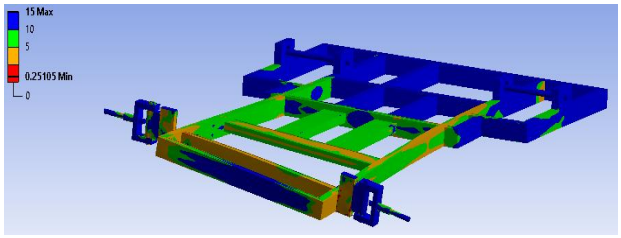

(b)

Figure 18: Deformation (a) and safety factor (b) of the seventh variation of chassis simulation

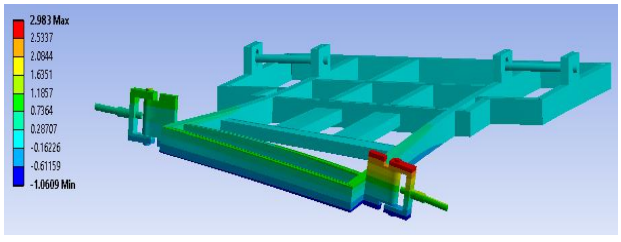

(a)

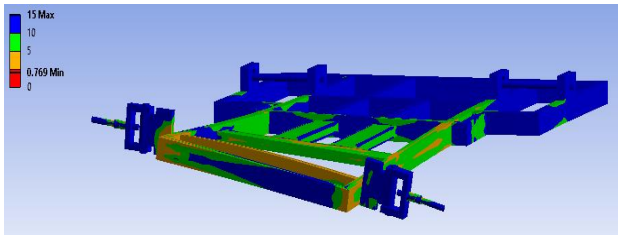

(b)

Figure 19: Deformation (a) and safety factor (b) of the eighth variation of chassis simulation

1.104 mm is derived from Figures 3 and 7. The minimum safety factor is 1.459, which is quite strong.

In the sixth variation of the chassis, a maximum deformation of 3.061 mm is obtained, and a minimum deformation of 1.109 mm, as seen in the color and matched with the legend in Figure 17. The minimum safety factor obtained from this variation is 1.484, which indicates that this chassis is quite substantial because the deformation is still above the yield strength value.

In the seventh variation, the chassis obtained a maximum deformation of 2.930 mm with a minimum deformation of 1.117 mm, as seen from color and matched with the legend in Figure 18. The minimum safety factor obtained from this variation is 0.251, which indicates that this chassis is not strong enough because the deformation is still below the value of 1.

In the eighth variation chassis, the maximum deformation is 2.983 mm, while the minimum deformation of 1.061 mm is seen in the color and matched with the legend in Figure 19. The minimum safety factor obtained from this variation of 0.769, which indicates that this chassis is not

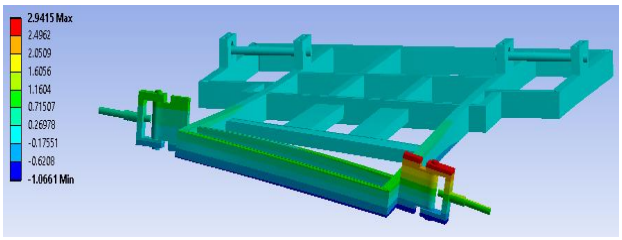

(a)

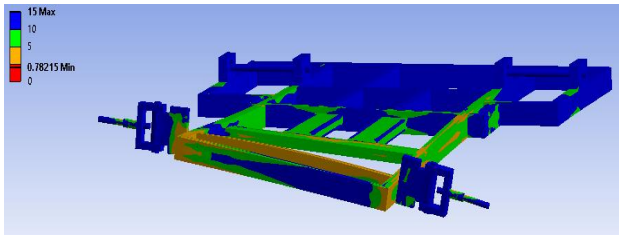

(b)

Figure 20: Deformation (a) and safety factor (b) of the ninth variation of chassis simulation

strong enough because the deformation is still below the value of 1.

In the ninth variation of the chassis, the maximum deformation of 2.942 mm and the minimum deformation of 1.066 mm are seen in the color and matched with the legend in Figure 20. The minimum safety factor obtained from this variation is 0.782, which indicates that the chassis is quite strong, because the deformation is still above the value of yield strength.

The results of the nine simulations show varying deformation and safety factor values. The total deformation value of the first variation chassis is 4.147 mm, and the safety factor is 0.336. In the second variation, the total deformation value is 4.141 mm, with a safety factor of 1.018. In the third variation, the total deformation value is 4.103 mm, with a safety factor of 1.036. The fourth variation has a total deformation value of 4.210 mm, with a safety factor of 0.476. The fifth variation has a total deformation value of 4.208 mm, with a safety factor value of 1.459. The sixth variation has a total deformation value of 4.170 mm with a safety factor of 1.484. In the seventh variation, a total deformation value of 4.046 mm was obtained, with a safety factor of 0.251. The eighth variation has a total deformation value of 4.044 mm, with a safety factor of 0.769. In the ninth variation, a total deformation value of 4.008 mm was obtained, with a safety factor of 0.782. The safety factor values for the second, third, fifth, and sixth chassis variations show safe results, which means that the stress of the simulation results is less than the yield strength of the material, and the design of the chassis can be considered safe [24]. The ideal

Table 9: Summary of the chassis deformation

Variation	Deformation (mm)	Deformation (deg)
1 (Al5 0.4)	4.1467	0.215002
2 (Al5 0.9)	4.1406	0.214686
3 (Al5 1.4)	4.1033	0.212752
4 (Al6 0.4)	4.2098	0.218273
5 (Al6 0.9)	4.2077	0.218165
6 (Al6 1.4)	4.1699	0.216205
7 (Al7 0.4)	4.0461	0.209786
8 (Al7 0.9)	4.0439	0.209672
9 (Al7 1.4)	4.0076	0.207790

chassis has high stiffness with minimal weight and price. Large deformation, when given a twisting load, causes the chassis to vibrate and the entire vehicle system is disturbed, meaning that handling performance will decrease [25].

The torsional load magnitude depends on the chassis dimensions (Eq. (1)) and the load distance from the center of the chassis (L), even with the same load (F). The simulation shows two different parameters to determine torsional stiffness, namely total deformation and safety factor. The deformation results are then calculated using Eq. (3), obtaining the torsional stiffness value. Deformation in the chassis is obtained by looking at the legend color shown in the simulation results. Then, the deformation results are calculated using Eq. (2) in order to change the deformation from the unit of length to the unit of degree. The deformation of each chassis variation is shown in Table 9.

5.2 Torsional stiffness

Torsional stiffness values are calculated by comparing the torque moment given to the deformation (Eq. (3)), where the results are shown in Table 10. Furthermore, the comparison between torsional stiffness to vehicle weight uses Eq. (5) and is shown in Table 11. It is known that the safety factor value of safe chassis design is found in the second, third, fifth, and sixth variations. The comparison value between torsional stiffness and its weight in the second variation is 311.59 Nm/deg.kg, and is 242.52 Nm/deg.kg for the third variation. Torsional stiffness in the third variation increases by approximately 21 Nm/deg from the second variation chassis because the deformation experienced is smaller, given the increased thickness of the chassis profile. The comparison value between torsional stiffness and its weight in the fifth variation is 304.35 Nm/deg·kg, and is 236.88 Nm/deg·kg in the sixth variation. Torsional stiffness in the sixth variation also increased by approximately 21 Nm/deg

Table 10: Calculation of the torsional stiffness

Variation	Twisting load (Nm)	Deformation (deg)	Torsional stiffness (Nm/deg)
1 (Al5 0.4)	497.2716	0.215002	2312.8718
2 (Al5 0.9)	497.2716	0.214686	2316.2790
3 (Al5 1.4)	497.2716	0.212752	2337.3350
4 (Al6 0.4)	497.2716	0.218273	2278.2052
5 (Al6 0.9)	497.2716	0.218165	2279.3420
6 (Al6 1.4)	497.2716	0.216205	2300.0041
7 (Al7 0.4)	497.2716	0.209786	2370.3773
8 (Al7 0.9)	497.2716	0.209672	2371.6669
9(Al7 1.4)	497.2716	0.207790	2393.1487

Table 11: Comparison of the torsional stiffness to the weight load

Variation	Torsional stiffness (Nm/deg)	Chassis weight (kg)	Torsional stiffness to weight ratio (Nm/deg·kg)
1 (Al5 0.4)	2312.8718	5.110	452.6398
2 (Al5 0.9)	2316.2790	7.434	311.5857
3 (Al5 1.4)	2337.3350	9.638	242.5188
4 (Al6 0.4)	2278.2052	5.148	442.5527
5 (Al6 0.9)	2279.3420	7.489	304.3457
6 (Al6 1.4)	2300.0041	9.710	236.8777
7 (Al7 0.4)	2370.3773	5.358	442.4326
8 (Al7 0.9)	2371.6669	7.794	304.2768
9 (Al7 1.4)	2393.1487	10.110	236.7110

from the fifth variation due to the same factors in the second and third variations [26, 27].

In the third variation, the torsional stiffness is 2337.33 Nm/deg, with a torsional stiffness-to-weight ratio of 242.52 Nm/deg kg. The ratio of torsional stiffness to weight decreases compared to the second variation, but it has a higher safety factor, indicating that the third variation is safer than the second variation. The chassis weight increases by about 2 kg, so the ratio of torsional stiffness to weight is lower. In the sixth variation, the torsional stiffness is 2300 Nm/deg, with a torsional stiffness-to-weight ratio of 236.88 Nm/deg kg. The ratio of torsional stiffness to weight decreases compared to the fifth variation, but it has a higher safety factor, which indicates that the sixth variation is safer than the fifth variation. The chassis weight increases by about 2 kg, so the ratio of torsional stiffness-to-weight is lower. Figure 21 shows the relationship between variations in each chassis material thickness with the torsional stiffness. It was found that the thicker the chassis used, the higher the torsional stiffness is. Changes in torsional stiffness also occur along with changes in the type of material used. The use of Al 7075 produces the highest torsional stiffness followed by Al 5052, and finally, Al 6061,

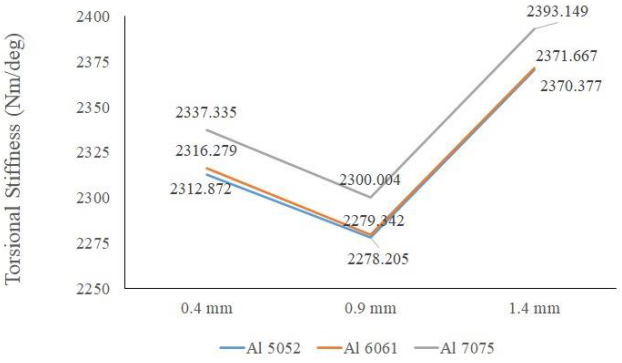

Figure 21: Relationship between chassis thickness and material type with the torsional stiffness

which is in line with Eq. (4), since Al 7075 has the highest shear modulus among the three materials [25].

Figure 22 shows the relationship between variations in each chassis' material thickness and the chassis weight. It was found that the thicker the chassis, the higher the chassis weight. This is caused by an increase in volume due to the thicker chassis. Changes in chassis weight also occur along with changes in the material used. The Al 7075 material produced the heaviest chassis, and the lightest is

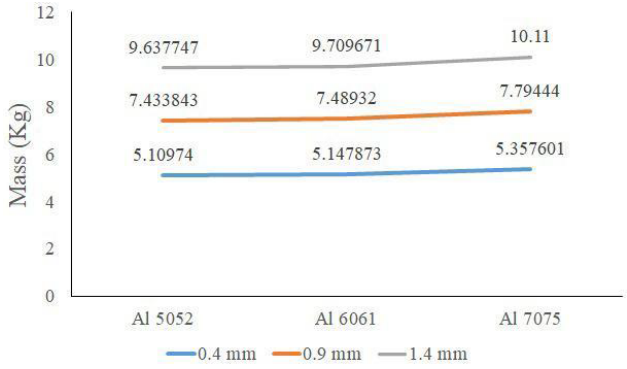

Figure 22: Relationship between chassis thickness and material type with the chassis mass

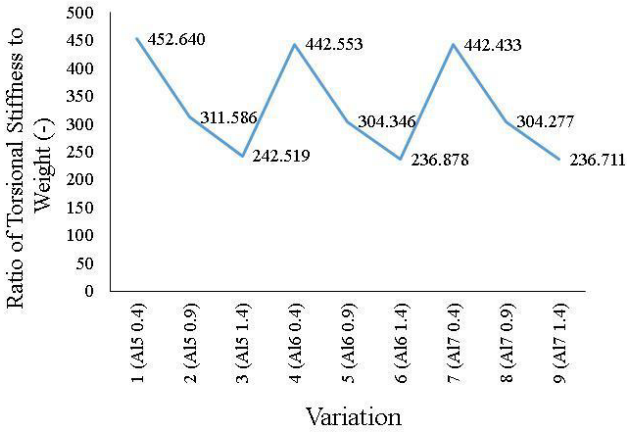

Figure 23: Ratio of torsional stiffness to the weight

Al 5052, as found in the material properties in Tables 5 to 7. This further implies that Al 7075 has the largest density, while the lowest density material is Al 5052.

Figure 23 shows the results of the ratio of torsional stiffness to the chassis weight. It can be seen that the first variation, namely the chassis with Al 5052 material and 0.4 mm thickness, has the largest ratio. In contrast, the ninth variation, with Al 7075 type material with 1.4 mm thickness, has the lowest ratio of all variations.

5.3 Comparison of the torsional stiffness to the reference criteria

In analyzing the safety of SEM urban vehicles, the safety factor (SF) of each variation will be analyzed first (based on the design and structure analyses of pioneer works [28–35]). Of the nine variations studied, four variations have sufficient SF values, namely the second, third, fifth, and sixth variations, with SF values of 1.02, 1.04, 1.46, and 1.48, respectively. The second and third variations use the Al 5052 material type (σ_Y = 193 MPa) with a thickness of 0.9 and 1.4 mm. The fifth and sixth variations use the Al 6061 material type (σ_Y = 275 MPa) with a thickness of 0.9 and 1.4 mm. In general, it can be seen that this result is mostly influenced by the material type, in particular the value of its yield strength, and is influenced less by its profile thickness.

After analyzing the SF of all variations, torsional stiffness is analyzed based on the reference criteria found in Subsection 4.1. Then, out of the four variations obtained from the SF analysis above, the third variation is decided to have the closest reference value for the SEM torsional urban vehicle stiffness, with a torsional stiffness value of 2.34 kNm/deg. The main factor that makes the third variation have the closest stiffness value to its reference value is the material type, Al 5052, which has a higher shear modulus than Al 6061.

6 Concluding remarks

The chassis for each variation was analyzed subsequently, and the deformation and the frame weight were obtained. The deformation results in the simulations are calculated to find the torsional stiffness. By incorporating these data into the calculation, the torsional stiffness to weight ratio of each variation was obtained. Based on calculations and analysis, it can be concluded that the strength of the SEM vehicle chassis can be obtained through simulations using ANSYS.

The design of each chassis variation has a relatively high torsional stiffness to weight ratio performance. However, only four variations have sufficient safety factor values, namely the second, third, fifth, and sixth variation. The factor which gives the most significant influence on the difference in torsional stiffness of each variation is the shear modulus of the material used. The weight of the chassis is influenced by the density of the material and the thickness of the chassis. In contrast, the safety factor of each variation is strongly influenced by the strength of the chassis structure itself. Mesh size for the variation affects the result of the chassis. Therefore, the first thing to do is calibrate the meshing size of the benchmark with the mesh size of the analysis for the optimum convergence result.

Finally, the conclusion is that the chassis which utilizes Al 5052 and 1.4 mm profile thickness for the frame has greater balance between performance and safety, while the most convergent mesh size could be seen at mesh size 15. Therefore, this type of chassis is the best variation to build.

Funding information: The authors state no funding involved.

Author contributions: All authors have accepted responsibility for the entire content of this manuscript and approved its submission.

Conflict of interest: The authors state no conflict of interest.

References

[1] Correira GH, Menendez M. Automated and connected vehicles: effects on traffic, mobility and urban design, Int. J. Transport. Sci Tech (Paris). 2017;6:iii–iv. https://doi.org/10.1016/S2046-0430(17)00025-9

[2] Rosero F, Fonseca N, López JM, Casanova J. Effects of passenger load, road grade, and congestion level on real-world fuel consumption and emissions from compressed natural gas and diesel urban buses. Appl Energy. 2021;282B:116195. https://doi.org/10.1016/j.apenergy.2020.116195

[3] Pandya B, El-Kharouf A, Venkataraman V, Wilckens RS. Comparative study of solid oxide fuel cell coupled absorption refrigeration system for green and sustainable refrigerated transportation. Appl Therm Eng. 2020;179:115597. https://doi.org/10.1016/j.applthermaleng.2020.115597

[4] Shell Eco-marathon. Shell Eco-Marathon The Neherlands 2019. Official Rules, Shell Eco-Marathon; 2019.

[5] Mat MH, Ghani AR. Design and analysis of "eco" car chassis. Proc Eng. 2012;41:1756–60. https://doi.org/10.1016/j.proeng.2012.07.379

[6] Airale A, Carello M, Scattina A. Carbon fiber monocoque for a hydrogen prototype for low consumption challenge. Materialwiss Werkstofftech. 2011;42(5):386–92. https://doi.org/10.1002/mawe.201100793

[7] Ary AK, Prabowo AR, Imaduddin F. Structural assessment of an energy-efficient urban vehicle chassis using finite element analysis – A case study. Procedia Struct Integr. 2020;27:69–76. https://doi.org/10.1016/j.prostr.2020.07.010

[8] Chapter 1. In: Vangi D. Structural Behavior of the Vehicle During the Impact - in Vehicle Collision Dynamics. Butterworth-Heinemann; 2020.

[9] Ubaidillah HH, Setiyawan AEP, Ramdhani HC, Saputra MZ, Imaduddin F. Vertical bending strength and torsional rigidity analysis of formula student car chassis. AIP Conf Proc. 2018;1931:030050. https://doi.org/10.1063/1.5024109

[10] Canut F, Malcher L, Henriques A. Structural analysis of a formula SAE chassis under rollover loads. 23rd ABCM Int Congr Mech Eng; 2015. https://doi.org/10.20906/CPS/COB-2015-0837

[11] Gaffney III EF, Salinas AR. Introduction to formula SAE suspension and frame design. SAE Tech Pap. 1997:971584. https://doi.org/10.4271/971584

[12] Siegler BP, Butler L, Deakin AJ, Barton DC. The application of finite element analysis to composite racing car chassis design [https://doi.org/10.1046/j.1460-2687.1999.00038.x]. Sports Eng. 1999;2(4):245–52.

[13] Riley WB, George AR. Design, analysis and testing of a formula SAE car chassis. SAE Tech Pap. 2002;18:2002-02-3300. https://doi.org/10.4271/2002-01-3300.

[14] Ary AK, Prabowo AR, Imaduddin F. Structural assessment of alternative urban vehicle chassis subjected to loading and internal parameters using finite element analysis. J. Eng. Sci. Tech. 2020;15:1999–2022.

[15] Douglas LM, William FM. Race Car Vehicle Dynamics. Society of Automotive Engineers Incorporation; 1996.

[16] Gao YF, Bower A. A simple technique for avoiding convergence problems in finite element simulations of crack nucleation and growth on cohesive interfaces [https://doi.org/10.1088/0965-0393/12/3/007]. Model Simul Mater Sci Eng. 2004;12(3):453–63.

[17] Velie HD. Chassis Torsional Rigidity Analysis for a Formula SAE Racecar. University of Michigan; 2016.

[18] Gawande SH, Muley AA, Yerrawar RN. Optimization of torsional stiffness for heavy commercial vehicle chassis frame [https://doi.org/10.1007/s42154-018-0044-6]. Auto Innov. 2018;1(4):352–61.

[19] Kurisetty P, Sukumar N, Gupta U. Parametric study of ladder frame chassis stiffness. SAE Tech Pap. 2016:2016-01-1328. https://doi.org/10.4271/2016-01-1328.

[20] Khoiron MS. Comparison of Strength and Strength of Chassis and Vehicle Body Made of Aluminum and Carbon Fiber Materials to Vertical and Torsional Bendings. Institut Teknologi Sepuluh Nopember; 2016. (*In Indonesian*).

[21] Chandan SN, Vinayaka N, Sandeep GM. Design, analysis and optimization of race car chassis for its structural performance [http://dx.doi.org/10.17577/IJERTV5IS070313]. Int J Engine Res. 2016;5:361–7.

[22] Singers MW. Chassis for Classic Car Vehicle Shell. University of New South Wales; 2009.

[23] Chinwuba IC. Timoshenko beam theory for the flexural analysis of moderately thick beams – variational formulation, and closed form solution [https://doi.org/10.18280/ti-ijes.630105]. Italian J. Eng. Sci. 2019;6(1):34–45.

[24] Nain R, Sharma R. Design and analysis of space frame tubular chassis to be used in formula SAE. Int. J. Aero. Mech. Eng. 2015;2:22–5.

[25] Armstead JK. Chassis Development for the Formula SAE Racer. University of Southern Queensland; 2006.

[26] Danielsson O, González CA, Ekström K, Bayani KM, Klomp M, Dekker R. Influence of body stiffness on vehicle dynamics characteristics. 24th Symp Int-Assoc Vehicle Syst Dynam. (IAVSD); 2015.

[27] Omer M. Design and Analysis of Composite Chassis for Shell Eco Marathon Prototype Vehicle 2016 using Finite Element Analysis. RWTH Aachen University; 2016.

[28] Koulocheris D, Vossou C. Exploration of equivalent design approaches for tanks transporting flammable liquids [10.3390/computation8020033]. Comp. 2020;8(2):33.

[29] Chapter 9. In: Aird P. Deepwater Well Design – in Deepwater Drilling. Gulf Professional Publishing; 2019.

[30] Caesar BP, Hazimi H, Sukanto H, Prabowo AR. Development of novel design and frame structural assessment on mitutoyo's auto checking hardness machine using reverse engineering approach: series hr-522 hardness tester, J. Eng. Sci Tech (Paris). 2020;15:1296–318.

[31] Findley DJ. Part 4 – Highway Geometric Design – in Highway Engineering. Butterworth-Heinemann; 2016.
[32] Ramsey JK. Calculating Factors of Safety and Margins of Safety From Interaction Equations, NASA Scientific and Technical Information (STI). Program; 2019.
[33] Prabowo AR, Bae DM, Cho JH, Sohn JM. Analysis of structural crashworthiness and estimating safety limit accounting for ship collisions on strait territory. Lat Am J Sol Struct. 2017;14:1594-1613. https://doi.org/10.1590/1679-78253942.
[34] DNV-GL. Standard for Offshore and Platform Lifting Appliances: Standard – DNVGL-ST-0378. Det Norske Veritas – Germanischer Lloyd; 2016.
[35] Charlton SG, de Pont JJ. Curve Speed Management – Research Report 323. Land Transport New Zealand; 2007.